ELSEVIER

Polymer 43 (2002) 2677–2689

polymer

www.elsevier.com/locate/polymer

Neutron scattering of hydrophobically modified poly(ethylene oxide) in aqueous solutions in the presence of latex particles

Emmanuel Beaudoin[a,*], Alain Lapp[b], Roger C. Hiorns[a], Bruno Grassl[a], Jeanne François[a]

[a]*Laboratoire de Physico-Chimie des Polymères, UPPA/CNRS UMR 5067, Hélioparc, 2 Avenue du Président Angot, 64053 Pau, France*
[b]*Laboratoire Léon Brilloin, CEA Saclay, 91191 Gif-sur-Yvette, France*

Received 2 April 2001; accepted 26 November 2001

Abstract

The structure of aqueous solutions of hydrophobically end-capped poly(ethylene oxide), PEOM, in the presence of solid particles (latex) was investigated by small angle neutron scattering. Mono- and di-functionalised PEOMs with the same ratio of hydrophilic to aliphatic ($C_{16}H_{33}$) hydrophobic groups of molecular weights 16 000 and 32 000 g mol^{-1}, respectively, were compared. We used solvent conditions in which either PEOM or latex were matched by varying the ratio of water to heavy water. Initially, a decrease in the scattering intensity at small angles was observed when PEOM was added to a suspension of latex at constant concentration. A peak was observed in the structure factor which indicated repulsion between particles. The position of the peak lied at a lower q value for mono-functionalised PEO than for di-functionalised PEO. This observation may be explained by the formation of bridges between aggregates by the di-functionalised PEOM. On varying the solvent, the characteristic peak of PEOM alone disappears at low polymer concentrations due to PEOM adsorption onto the latex particles but reappears at higher polymer concentrations.

Keywords: Associative polymers; Hydrophobically end-capped poly(ethylene oxide); Polystyrene latex

1. Introduction

Associative polymers consisting of hydrophilic poly (ethylene oxide), PEO, chains functionalised with one or two aliphatic end-groups, α or α,ω-modified PEOM, auto-associate in aqueous solutions to form micelles [1–4]. We have recently considered the synthesis and characterisation of model systems consisting of polymers with low molecular weight distributions and well controlled degrees of functionalisation [5–10]. In these systems, it is possible to clearly identify a critical association concentration above which micelle-like hydrophobic nano-domains are formed. At higher concentrations, 1–2%, a liquid order appears as shown in Fig. 1. Many experiments have already been performed by neutron [5,6], X-ray [7] and light scattering [8–10] which has yielded a good description of the organisation (cubic type), size and shape of the hydrophobic, spherical nano-domains. We have systematically studied their evolution while varying their intrinsic parameters (the length of PEO chains and of aliphatic groups and the polymer architecture whether linear, star- or comb-like [11]) and extrinsic parameters such as temperature and ionic strength.

From a practical point of view, the polymers described earlier are used as rheology modifiers of suspensions of latex, mineral particles and globular proteins in coatings, paints, or cosmetologic formulations. Several articles [12–15] have shown that associative polymers adsorb strongly onto hydrophobic latex surfaces through hydrophobic interactions—which are the dominant forces—but also through hydrogen bonds between un-ionised carboxylic acid groups which are present on the latex surface and the oxygen atoms of the hydrophilic PEO backbone [16]. The smaller the latex particle size, the greater this association is [17]. Smaller latex particles favour the adsorption of alkyl end-groups, rather than PEO backbone, as steric constriction occurs with the lower available adsorption surface area.

At low or moderate concentrations PEOM can flocculate latex by volume restriction, or by bridging when with di-functionalised PEO [17]. Stabilisation of the polymer at higher concentrations is explained by the formation of a homogeneous transient network of PEOM and latex [18,19]. To our knowledge, no experimental studies of the structure of such networks have yet been performed and it seemed interesting to know how the well-demonstrated adsorption phenomenon would modify polymer organisation.

Latices contain surfactants that stabilise dispersions. Depending on their concentration and nature, whether

* Corresponding author.

0032-3861/02/$ - see front matter
PII: S0032-3861(01)00817-5

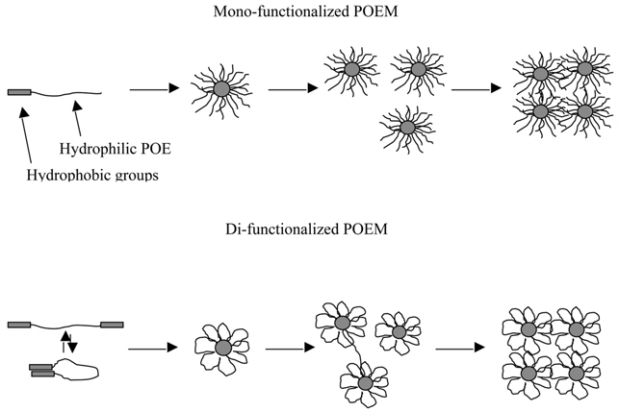

Fig. 1. Schematic representation of PEOM association in water.

non-ionic or ionic, surfactants can interact with PEOM in solution as well as compete with PEOM in the adsorption mechanism. It has been observed that addition of surfactants can increase as well as decrease viscosity [20], according to their concentration, latex size and surface acidity. Besides, if inter-particle bridging and a consequent increase of viscosity can be reasonably expected with α,ω functionalised PEO, mono-functionalised PEO must lead only to latex stabilisation through adsorption phenomenon. Thus, it would be very interesting to compare these two types of polymers. To make such a comparison significant, mono- and di-functionalised polymers of molecular weights 16 000 and 32 000, respectively, were used, thus giving the same hydrophilic/hydrophobic balance.

In this paper, we present small angle neutron scattering (SANS) experiments of the ternary systems PEOM (mono- and di-functionalised)/polystyrene latex/water. These systems were investigated in pure water and under conditions where either latex particles or PEOM could be matched in water/heavy water mixtures.

2. Experimental

2.1. Materials

2.1.1. Preparation of hydrophobically end-capped PEOM

α,ω functionalised PEO, D32C16. D32C16 was synthesised according to a method which differs slightly from that given by Kaczmarski and Glass [21].

Hexadecyl isocyanate was reacted with the hydroxyl chain-ends of α,ω-hydroxylated PEO (Fluka) in the presence of 1,4-diazabicyclo[2,2,2]octane, DABCO, according to the following experimental conditions [10]. Thirty grams of α,ω-hydroxylated PEO was purified by dissolving in toluene and precipitating in ether and was then dried under vacuum. The reaction vessel was dried and kept under nitrogen before and during use in order to eliminate traces of water, which react with the isocyanate. Toluene (90 ml) used as solvent was heated at 80 °C over sodium prior to being cryo-distilled into a 500 ml three necked flask. PEO was introduced under nitrogen and the mixture was heated to 60 °C until the PEO completely dissolved. DABCO (1% w/w with respect to the polymer) and an excess of hexadecyl isocyanate ($n = 3.8 \times 10^{-3}$ mol, 200% with respect to the PEO chain-ends) were introduced. The reaction medium was maintained at 60 °C for 240 h in order to obtain a 100% functionalisation. The hot reaction mixture was then filtered so as to eliminate reaction by-products (urea) and diluted in toluene to 10% w/w. The resultant polymer was precipitated in ether and recrystallised twice from toluene.

The weight average molecular weight of the PEO precursor was determined, by UV spectroscopy [10,22,23] and static light scattering (SLS), to be $\bar{M}_w = 32\,000$ and the molecular weight distribution, $\bar{M}_w/\bar{M}_n$, measured by size exclusion chromatography (SEC), was found to be 1.02. Since there is no indication of degradation occurring during the chemical modification of PEO [23], we will consider that the $\bar{M}_w$ of D32C16 is also 32 000.

α-functionalised PEO (M16C16). It should be noted that by using the same type of reaction on commercial samples of PEO as described earlier, it is possible to prepare only α-methylated, ω-hexadedylated PEO starting from α-methylated, ω-hydroxylated PEO (Me-PEO-OH). No Me-PEO-OH is commercially available with a molecular weight $\bar{M}_w = 16\,000$, half of that of D32C16. Moreover, it seemed better to have a polar function at one of the chain-ends, and prepare therefore a sample of the type $CH_3(CH_2)_{15}$ PEO-OH, in order to avoid the presence of a methyl chain-end hydrophobic group.

It was thought therefore that the most effective and least expensive route to poly(ethylene oxide) mono-hexadecyl ether would be via the anionic polymerisation of ethylene oxide using the initiator potassium hexadecyloxide.

THF and toluene were distilled over their respective drying agents under predried nitrogen prior to use. The preparation of potassium hexadecyloxide was performed under predried nitrogen. The polymerisation of ethylene oxide was performed using standard high vacuum techniques [24]. Ethylene oxide was distilled under vacuum into break-seals of predetermined size; 1-hexadecanol, acidified methanol, and 18-crown-6 were also transferred into break-seals of predetermined size and sealed under high vacuum. Methanol, hydrochloric acid (37% solution in water) and 18-crown-6 were used as received. All of the above chemicals were supplied by Aldrich®.

2.1.1.1. Synthesis of potassium hexadecyloxide. Into a flame dried and nitrogen flushed *Schlenk* tube was placed excess potassium (1 g, 0.026 mol) and THF (100 ml). 1-hexadecanol (0.25 g, 1.03×10^{-3} mol) was then added and dissolved into the THF at room temperature. With stirring, a white precipitate of potassium hexadecyloxide slowly formed. After 18 h, the precipitate was left to settle and the THF was removed via syringe. The remaining solid lumps of

potassium were carefully removed with tweezers. The resulting fine white powder was dried under vacuum for 18 h (yield near 100%).

2.1.1.2. Synthesis of poly(ethylene oxide) mono-hexadecyl ether. A 250 ml reactor fitted with a magnetic stirring bar, magnetic breakers and break-seals containing ethylene oxide (13.6 ml, 12 g, 0.272 mol), potassium hexadecyloxide (0.160 g, 5.70×10^{-4} mol), excess 18-crown-6 (0.3 g, 1.14×10^{-3} mol) and acidified methanol (2 ml) was evacuated and flame dried. Once THF (200 ml) was distilled into the vessel, it was then sealed under high vacuum. Potassium hexadecyloxide and 18-crown-6 were introduced and dissolved into the THF with stirring at 70 °C for 36 h. The solution was then cooled to 30 °C and the ethylene oxide was introduced (*extreme care*: the ethylene oxide was cooled with liquid nitrogen prior to its break-seal being opened, as otherwise the ethylene oxide may have expanded rapidly causing an explosion of the reaction vessel). For the first 24 h, the solution was stirred at 50 °C. After which the solution was stirred for 178 h at 70 °C. Acidified methanol was introduced to the solution at room temperature to terminate the reaction. The solution became visibly more viscous with the formation of hydroxy chain-end groups.

The polymer was precipitated twice from THF (200 ml) into diethyl ether (800 ml). The resulting fine white powder was collected by centrifuge and dried under vacuum at room temperature for 72 h with yield 10.9 g (91%).

2.1.2. Characterisation of hydrophobically end-capped PEOM

2.1.2.1. ^1H NMR. Samples were dissolved in a 50/50 mixture of $CDCl_3$ and DMSO and filtered prior to characterisation in order to fully solvate both the PEO chain and chain-ends. ^{1}H (400 MHz) NMR spectra were recorded on a Bruker AM-400 spectrometer. Residual hydrogen in $CDCl_3$ was used to reference ^{1}H shifts.

^{1}H NMR can be used to determine both the degree of functionalisation and the polymer's molecular weight. The degree of functionalisation, τ, of D32C16 was indicated by ^{1}H NMR (see Fig. 2(a)) by using a internal probe (hexamethyl cyclotrisiloxane) [10,23] of the main PEO chain: $\tau = 100\%$.

Characterisation of M16C16 by ^{1}H NMR (see Fig. 2(b)) indicated, by integration, that there was the expected 3/1 ratio of methyl (0.8 ppm) to hydroxy (4.4 ppm) protons of the polymer end-groups. The relative ratio of end-groups to ethylene protons (3.5 ppm) indicated the polymer to have $\bar{M}_n = 15\,500$.

2.1.2.2. Size exclusion chromatography. Molecular weights of M16C16 was obtained relative to polystyrene standards using SEC equipment supplied by Waters®. Determinations were carried out at 40 °C using a bank of four columns (HR 0.5, 2, 4 and 6®) of 300 mm × 5 μm Styragel® with an ERC® INC 7515A refractive index (RI) detector. THF was used as eluent at a flow rate of 1.0 ml min^{-1} using a Waters® 2690 pump.

SEC analysis indicated that the polymer's mass was higher than that obtained by ^{1}H NMR. ($\bar{M}_n = 20\,640$, $\bar{M}_w/\bar{M}_w = 1.06$). This discrepancy may be explained by an error introduced by the SEC as it was calibrated relative to polystyrene standards and not those of poly(ethylene oxide).

2.1.3. Latex preparation

Polystyrene latex, PS1 (10% w/w) was synthesised by radical polymerisation in emulsion in 200 ml bulk. Potassium persulfate (Aldrich) was used as initiator. Sodium dodecyl sulfate (SDS; 1% w/w with respect to the monomer) was used as stabiliser, no other surfactant was added. Dynamic light scattering (DLS) measurements indicated a hydrodynamic diameter of 90 nm.

Some measurements were also made with commercial PS latex from Sigma, PS2 (10% weight concentration, not assayed by Sigma).

2.1.4. Latex characterisation

Latex was characterised by two different light scattering methods:

using classical DLS on highly diluted latex suspension (0.01% w/w) using a goniometer from Sematech with a He–Ne laser source (wavelength 632 nm);
using an apparatus just recently developed (DL 135-45, Sematech, IFP, France) permitting size particle measurements from thin layers of opaque and coloured solutions and suspensions [25]. It was recently demonstrated that the true size of particles can be determined up to concentrations of about 20% [26,27].

Both techniques gave hydrodynamic radii of 90 ± 5 and 80 ± 5 nm for PS1 and PS2, respectively. In the latter case, this result is in agreement with the value of 91 nm (±6 nm) given by Sigma.

2.2. Small angle neutron scattering

SANS experiments were performed on PAXY spectrometer at Léon Brillouin Laboratory (LLB; CEA, Saclay, France). Scattering ranges covered were $0.003 < q$ (Å^{-1}) < 0.022 and $0.018 < q$ (Å^{-1}) < 0.09. Samples were at 20 °C.

The scattered intensity $I(Q)$ for a solution or solvent is given by:

$$I(q) = \frac{\left(\frac{I_s}{(eT_s)} - \frac{I_{cv}}{(eT_{cv})}\right)}{\left(\frac{I_{water}}{(eT_{water})} - \frac{I_{cv}}{(eT_{cv})}\right)} \times \left(\frac{d\Sigma}{d\Omega}\right)_{water} \quad (1)$$

where $(d\Sigma/d\Omega)_{water}$ is the effective section of water, e is the

(a)

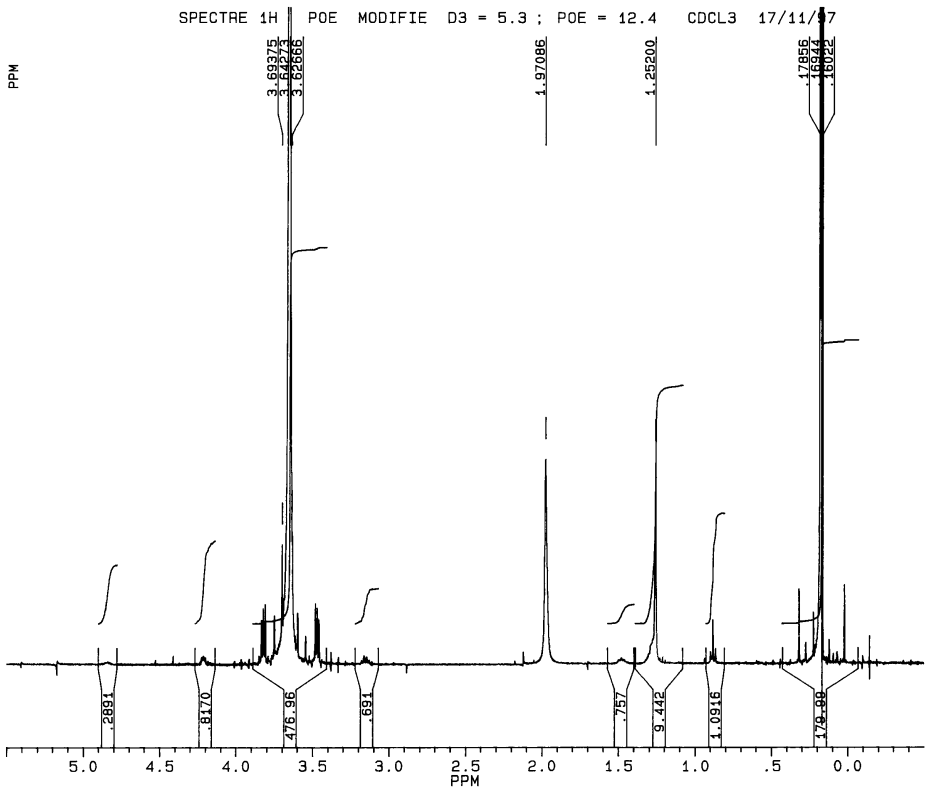

1H NMR of C16N32

(b)

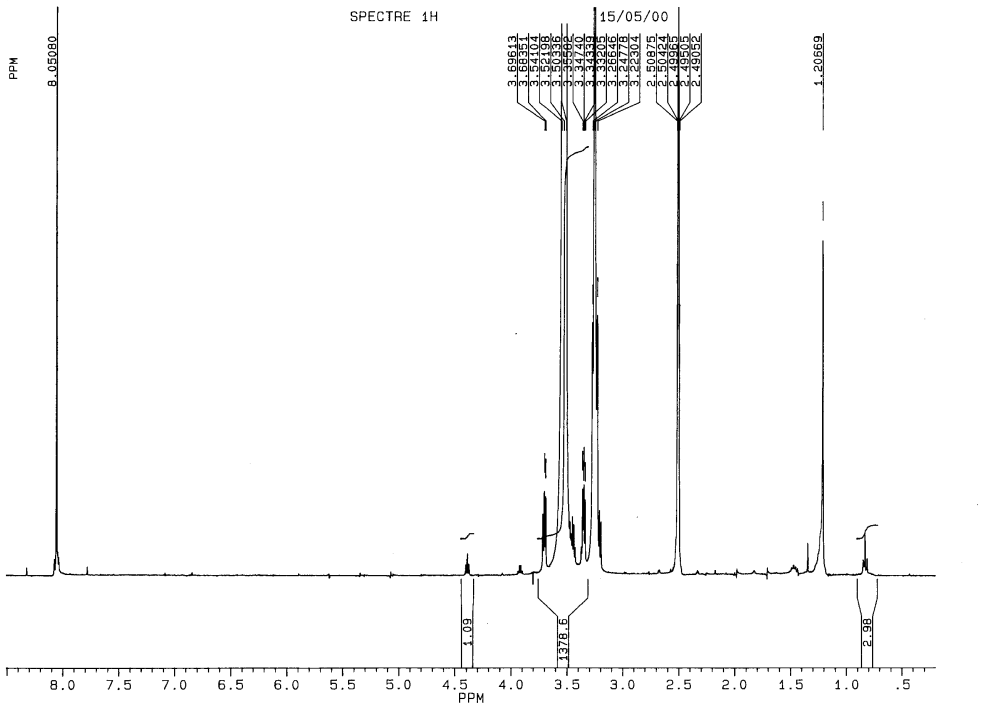

1H NMR of MC16

Fig. 2. [1]H NMR spectra of (a) D32C16 and (b) M16C16.

Table 1
Length scattering densities of different constituents

Unit	PEO	PS	D_2O	H_2O	CH_2	CH_3
ρ (cm Å^{-3})	0.66	1.40	6.38	−0.56	−0.31	−1.03

cell thickness, I_s, I_{cv} and I_{water} are the scattered intensity of the sample, the empty cell and water, respectively. T_s, T_{cv} and T_{water} are the transmitted intensity of the sample, the empty cell and water, respectively.

The coherent contribution ΔI of a solute can be calculated from the intensity scattered by the solution $I(q)_{solution}$, that scattered by pure solvent $I(q)_{solvent}$, the solute volume fraction Φ_p and the incoherent contribution of the solute I^{inc}.

$$\Delta I = I(q)_{solution} - (1 - \Phi_p)I(q)_{solvent} - \Phi_p I^{inc}(q) \quad (2)$$

The incoherent contribution of PS and PEOM were determined in water/heavy water mixtures where their coherent contribution is matched.

ΔI can be described by the form factor $P(q)$ and the structure factor $S(q)$, which are, respectively, related to the form and size and to the structure of the scattering centres.

$$\Delta I = \Delta\rho^2 N V^2 P(q) S(q) \quad (3)$$

where $\Delta\rho^2 = (\rho_{polymer} - \rho_{solvent})^2$ is the contrast factor, N, the number of molecules and V is the volume of the molecules.

Table 1 gives the length scattering densities of the different chemical species or units present in the characterised systems.

By varying the proportion of water and heavy water, we could change the contrast of the solvent and match either polymer or latex particles. We used three solvent conditions (Fig. 3):

Pure water: nothing is matched.
Mixture of H_2O/D_2O (28.3% D_2O): latex particles are matched, ΔI represents only the contribution of PEOM.
Mixture of H_2O/D_2O (17.6% D_2O): PEOM is matched, ΔI represents only latex particles scattering.

2.2.1. Preparation of the solutions

Polymer concentrations were 3, 5, 10 and 20% (w/w), and latex concentrations were 1 and 10% (w/w).

Polymer solutions with a 10% latex concentration in 100% H_2O were prepared directly by dissolving the polymer into a latex suspension. Preparing polymer/latex solutions in H_2O/D_2O mixtures (28.3% D_2O or 17.6% D_2O) required the 10% latex solutions to be concentrated up to 14% by evaporating water, and then readjusted to 10% latex with the right amount of D_2O.

Other latex concentrations are made by diluting latex with 3× (2× on quartz) distilled water, filtered to 0.1 μm before proceeding as described later.

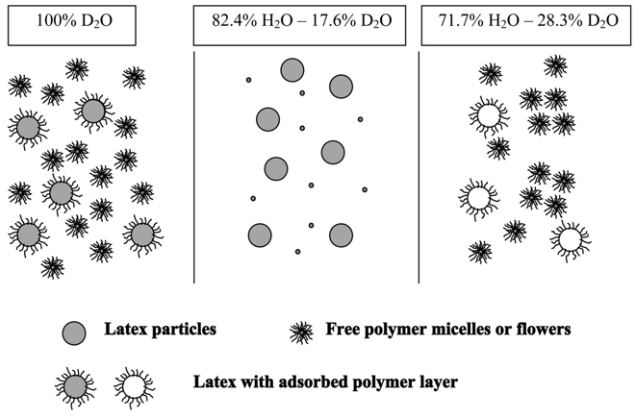

Fig. 3. Matching conditions of SANS experiments.

3. Results

3.1. Latex suspension in water

The scattered intensity curve (ΔI) for pure PS1 latex in H_2O at 1% is shown in Fig. 4. It exhibits the small oscillations expected for hard spheres. The structure factor, $S(q)$, at such a concentration may be neglected in the first instance: $S(q) = 1$ in Eq. (3). The form factor, $P(q)$, for monodisperse hard spheres of radius R is [28]:

$$P(q) = \left(\frac{3}{u^3}(\sin u - u\cos u)\right)^2 \quad (5)$$

where $u = qR$, q is the wave vector ($q = (4\pi/\lambda)\sin(\theta/2)$, where θ is the scattering angle).

The curve calculated according to Eqs. (3) and (5) has oscillations considerably more pronounced than those found by experiment (Fig. 4). The attenuation of the oscillations can be attributed to a polydispersity effect.

In the case of polydisperse hard spheres, the average form factor $P'(q)$ is

$$P'(q) = \sum_0^\infty P(q,R)D(R) \quad (6)$$

where $D(R)$ is the distribution function of the particle radii. The Schulz–Zimm distribution with an average radius $\langle R\rangle$ was used:

$$D(R) = \frac{k^k}{\Gamma(k)}\frac{R^k}{\langle R\rangle^{k+1}}\exp\left(\frac{-kR}{\langle R\rangle}\right) \quad (7)$$

This leads to a better description of our system with $k = 50$, meaning a polydispersity index I_p of $(k+1)/k = 1.02$. However, the best fit is obtained for a particle diameter of 80 nm, slightly smaller than the measured hydrodynamic radius (90 nm).

In the second instance, we tried to fit the experimental curves using both from the factor, $P'(q)$, and the structure

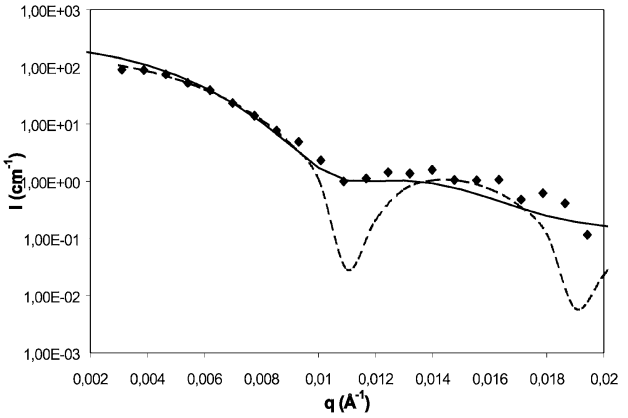

Fig. 4. Scattered intensity (ΔI) for a pure latex suspension (◆: 1% PS1). Fit with form factor of monodisperse spheres (- - -) (relations (5) and (6)) and polydisperse spheres (—) (relations (6) and (7); structure factor ($S(q) = 1$ in relation (3)).

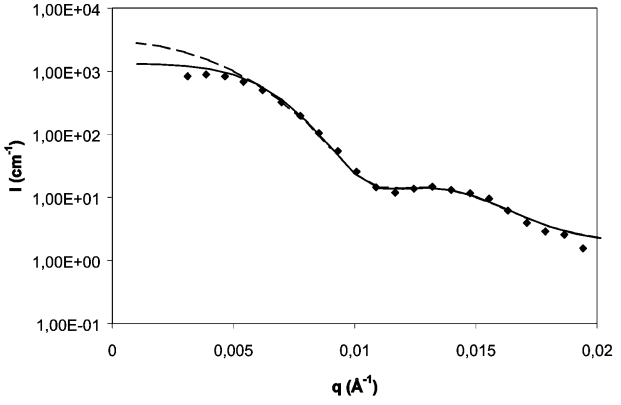

Fig. 5. Scattered intensity (ΔI) for a pure latex suspension (◆: 10% PS1). Fit with form factor of polydisperse spheres (- - -) and with the product of a form factor by the structure factor given by relations (11)–(13) (—).

factor, $S(q)$:

$$S(q) = N\left[1 + N\int_0^\infty g(r)\frac{\sin qr}{qr}4\pi r^2\,\mathrm{d}r\right] \tag{8}$$

$S(q)$ has been calculated for monodisperse hard spheres with an Ornstein–Zernicke approximation of Fourier transform $g(q)$ of $g(r)$:

$$g(q) = \frac{C(q)}{1 - NC(q)} \tag{9}$$

$C(q)$ is Fourier transform of direct correlation function $C(r)$, calculated from Percus–Yevick approximation [29]:

$$C(r) = -\alpha - \beta\left(\frac{r}{2R}\right) - \gamma\left(\frac{r}{2R}\right)^3 \tag{10}$$

where α, β and γ are functions of the volume fraction Φ:

$$\alpha(\Phi) = (1 + 2(\Phi))^2/(1 - \Phi)^4,$$

$$\beta(\Phi) = -6\Phi(1 + \Phi/2)^2/(1 - \Phi)^4, \tag{11}$$

$$\gamma(\Phi) = (\Phi/2)(1 + 2\Phi)^2/(1 - \Phi)^4$$

$$S(q) = \left[1 + 24\Phi\frac{G(2qR\Phi)}{2qR}\right]^{-1} \tag{12}$$

$G(u, \Phi)$ is a trigonometric function of hard sphere radius R and $y = qR$

$$\begin{aligned} G(u,\Phi) = {} & (\alpha(\Phi)/4u^2)[\sin(2u) - 2u\cos(2u)] + (\beta(\Phi)/8u^3) \\ & \times [4u\sin(2u) + (2 - 4u^2)\cos(2u) - 2] \\ & + (\gamma(\Phi)/32u^5)[-16u^4\cos(2u) + 4[(12u^2 \\ & - 6)\cos(2u) + (8u^3 - 12u)\sin(2u) + 6]] \end{aligned} \tag{13}$$

The structure factor can then be calculated analytically and the scattered intensity can be deduced from Eq. (3).

No improvement was seen on the 1% concentration latex curves, which proved that no repulsion between particles occurs at this concentration. However, scattering intensity is best described using both $P(q)$ and $S(q)$ with a 10% latex concentration (Fig. 5).

3.2. Polymers in heavy water

D_2O is generally chosen for studying PEOM or PEO because of the higher contrast factor it shows with respect to water.

The scattering curves obtained for di-functionalised PEOM in heavy water are given in Fig. 6 at different polymer concentrations. They exhibit one broad peak at low q values, as already described for other associating polymers [5,6] with shorter end-groups (aliphatic chains of 12 carbon atoms). It reflects the existence of a liquid-like order. Sometimes, a shoulder appears at higher q values. The ratio of the maximum of the main peak to that of the shoulder, q_1/q_2, was found to be close to $1/\sqrt{3}$, a value expected for the first to third order of a cubic array. Since, by decreasing the

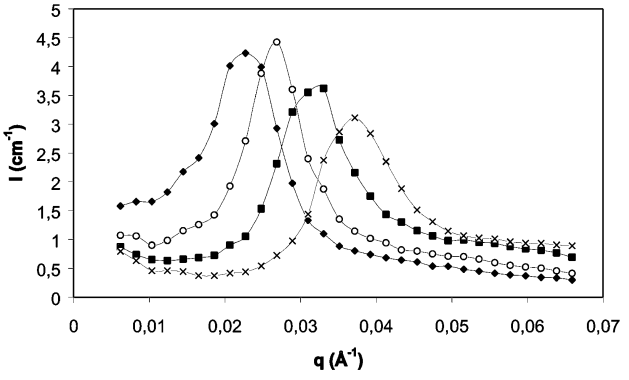

Fig. 6. Scattered intensity for different concentrations of di-functionalised PEO, D32C16 (◆: 3%, ○: 5%, ■: 10%, ×: 20%).

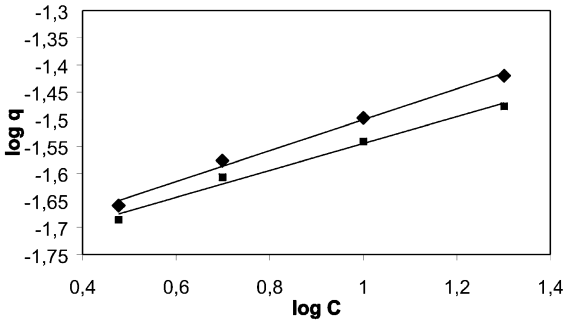

Fig. 7. Logarithm plot of the scattering vector at the peak maximum versus polymer concentration: D32C16 (◆); M16C16 (■).

length of the PEO chain, SAXS patterns clearly corresponds to either a primitive cubic (p.c.) or a body centred cubic (b.c.c.) [7], with up to six Bragg peaks, it could be concluded that this corresponded to the presence of a cubic liquid order, even when only one peak is present in the scattering curves. This is probably the case for the D32C16 under study. As seen in Fig. 6, the position of the peak q_{max} is shifted towards higher q values when concentration increases. A logarithm plot of q versus polymer concentration C_p (Fig. 7) gives a power law:

$$Q_{max} \propto C_p^{0.29} \tag{14}$$

The same results were qualitatively obtained with M16C16, which indicates the same structure for both systems, but the exponent is slightly lower (0.24), as shown in Fig. 7. In fact, a 1/3 exponent was expected for a system which is concentrated without changes in the micelles size. Nevertheless, these results are in agreement with those previously found [5,6], and show that the systems display a general behaviour. It indicates that the aggregation number increases upon increasing polymer concentration and will be discussed elsewhere.

In a mixture of H_2O/D_2O (17.6% D_2O), where only the hydrophobic nano-domains contribute to neutron scattering, the intensity of the peak maximum (I_{max}) increases with increasing concentration. When the PEO chains are not matched, the correlation peak intensity increases only up to the concentration where the 'flowers' overlap C^* and then decreases as seen in Fig. 6. At very high concentrations above C^*, the system behaves almost as a semi-dilute solution of PEO, without a correlation peak. This effect will be described in detail in the future paper.

3.3. Latex and polymer solutions

3.3.1. Preliminary remarks

1. Light scattering experiments have already been performed on these ternary systems [30]. They showed that the size of the particles increases when M16C16 or D32C16 are added to a latex suspension of 1%. The fact that a plateau in the variation of the size versus polymer concentration is reached at more than 10% w/w of polymer with respect to the latex suggested an adsorption phenomenon, this threshold corresponding to the saturation of the latex surface. Nevertheless, as discussed elsewhere, the observed increase in the particle size is much higher with PS latex than that expected for a polymer monolayer [30]. Measurements of the adsorption isotherms are in progress.
2. We have attempted to establish phase diagrams with this ternary system: PS1 (and PS2)/D32C16/H_2O: with 10% latex, and a visual observation only indicates inhomogeneities in the mixtures at very low polymer concentration ($C_p < 0.1\%$) or at concentrations higher than 20%.
3. Observations with an optical microscope of the systems investigated by neutron scattering do not indicate presence of aggregates of sizes greater than 1 μm.

The neutron scattering experiments were performed by keeping the latex concentration constant (at 1 and 10%) and varying the polymer concentration between 1 and 20%.

3.3.2. Pure water solutions

In pure water solutions, the latex particles are seen most clearly as their contrast is higher than that of PEOM. Yet, the scattered intensity is the sum of different terms from latex and PEOM. Even when neglecting the aliphatic endgroups of PEOM, the scattered intensity can be expressed as the sum of three terms where ρ and Φ are, respectively, the length scattering density and the volume fraction of the different constituents: PEO, latex or solvent according to the indices:

a first term corresponding to the PEO contribution: $(\rho_{PEO} - \rho_{solvent})^2 \Phi_{PEO} G_1(Q)$ where $G_1(Q)$ is the scattering function of PEO. The contrast factor of PEO with respect to water is $(\rho_{PEO} - \rho_{solvent})^2 = (\Delta\rho_1)^2 = 1.488\ cm^{-1}$;

a second term corresponding to the latex contribution: $(\rho_{latex} - \rho_{solvent})^2 \Phi_{latex} G_2(Q)$ where $G_2(Q)$ is the scattering function of the latex. The contrast factor of latex with respect to water is $(\rho_{latex} - \rho_{solvent})^2 = (\Delta\rho_2)^2 = 3.842\ cm^{-1}$;

a third crossed term: $2(\rho_{PEO} - \rho_{solvent})(\rho_{latex} - \rho_{solvent})\Phi_{PEO}\Phi_{latex} G_1(Q)G_2(Q)$ with a contrast factor $2(\rho_{PEO} - \rho_{solvent})(\rho_{latex} - \rho_{solvent}) = 2(\Delta\rho_1)(\Delta\rho_2) = 4.782\ cm^{-1}$.

Length scattering densities are given in Table 1.

Without any interaction between PEOM and latex, $G_1(Q)$ and $G_2(Q)$ are expected to remain constant. As the crossed term is positive, adding polymer at a constant latex concentration should result in an increase of the scattered intensity, as Φ_{PEO} increases. However, Fig. 8 shows a strong drop of the scattering intensity in a wide q range with a constant 10% latex concentration. This clearly demonstrates that interactions between PEOM and latex occur. As a

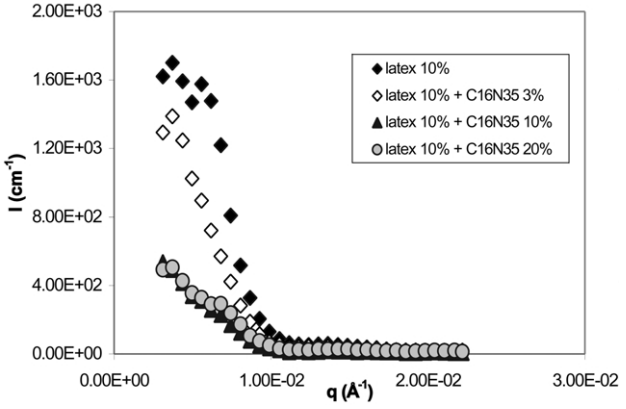

Fig. 8. Scattered intensity of 10% PS1 latex suspension in pure water (◆) and in the presence of 3% (◇), 10% (▲) and 20% (◍) of D32C16.

consequence, adding polymer clearly decreases the concentration fluctuations in the solution.

The first idea consists in considering that the adsorption of polymer forms, at the latex surface, a repulsive layer, since the solvent is good for the polymer.

3.3.3. H_2O/D_2O (71.7/28.3%) as solvent

In using a mixture of H_2O and D_2O as the solvent, the latex particles are matched and only the PEOM is measured.

In Fig. 9, one can compare pure D32C16 solutions and D32C16/latex with PS2 latex at the same polymer concentrations. In fact, measurements on pure D32C16 solutions were made only in 100% D_2O in order to gain the greatest contrast. For a significant comparison of polymer behaviour in the binary and ternary systems, the scattered intensities in the mixture I_{mixture} was calculated from that measured in 100% D_2O (I_{D_2O}) taking into account the differences in contrast factor in the two different solvents:

$$I_{\text{mixture}} = \frac{(\rho_{\text{PEO}} - \rho_{\text{mixture}})^2}{(\rho_{\text{PEO}} - \rho_{D_2O})^2} I_{D_2O} \tag{15}$$

where ρ_{mixture} and ρ_{D_2O} are, respectively, the scattering length densities of the H_2O/D_2O (71.7/28.3%) mixture and heavy water.

Fig. 9(a) and (b) correspond to measurements made with 10% latex and, respectively, 3 and 10% (w/w with respect to the solvent) D32C16. At the lower polymer concentration, the characteristic peak of the polymer, which appears in heavy water at $q_{\max} = 0.023$ Å^{-1}, is replaced in the mixed solvent by a shoulder at a smaller scattering vector ($q_{\max} = 0.018$ Å^{-1}). This indicates that a non-negligible part of the polymer, probably adsorbed onto the latex, does not participate in the formation of the flower network. However, in the case of the 10% polymer solution, the calculated and measured curves are superimposed, which is not really surprising since, in the hypothesis of polymer adsorption, the adsorbed fraction becomes negligible with respect to the total amount of polymer.

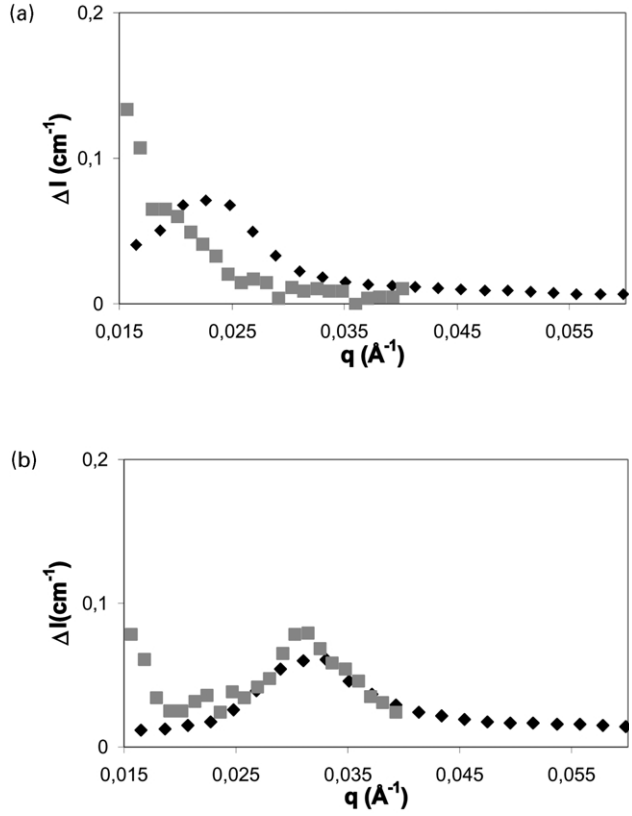

Fig. 9. Scattered intensity of (a) 3% and (b) 10% di-functionalised alone (◆) and PEO in the presence of 10% PS1 latex particles (■) in H_2O/D_2O (71.7/28.3%) mixture.

(i) In the case of the 3% polymer solution, one may assume that the shoulder is due to non-adsorbed polymer. As the position of the polymer peak in pure water varies with $C_p^{1/3}$, one could deduce that half the initial concentration is adsorbed onto the latex, i.e. 0.015 g ml^{-1}. This value is close to the value of polymer concentration at which the latex is saturated by polymer obtained by DLS (0.01 g ml^{-1}).

From this last value, one can calculate available latex surface per polymer molecule (S_{pl}) for 10% latex. Considering that 1 g ml^{-1} of polymer is adsorbed:

$$S_{\text{pl}} = \frac{4\pi R^2 N_{\text{l}} \bar{M}_{\text{w}}}{C_{\text{p}} N_{\text{a}}} \tag{16}$$

where the total number of latex particles per unit volume N_{l} is calculated from:

$$N_{\text{l}} = \frac{C_{\text{l}}}{\frac{4\pi}{3} R^3 d_{\text{l}}} \tag{17}$$

for a total number of macromolecules per unit volume which is:

$$N_{\text{p}} = \frac{C_{\text{p}} N_{\text{a}}}{\bar{M}_{\text{w}}} \tag{18}$$

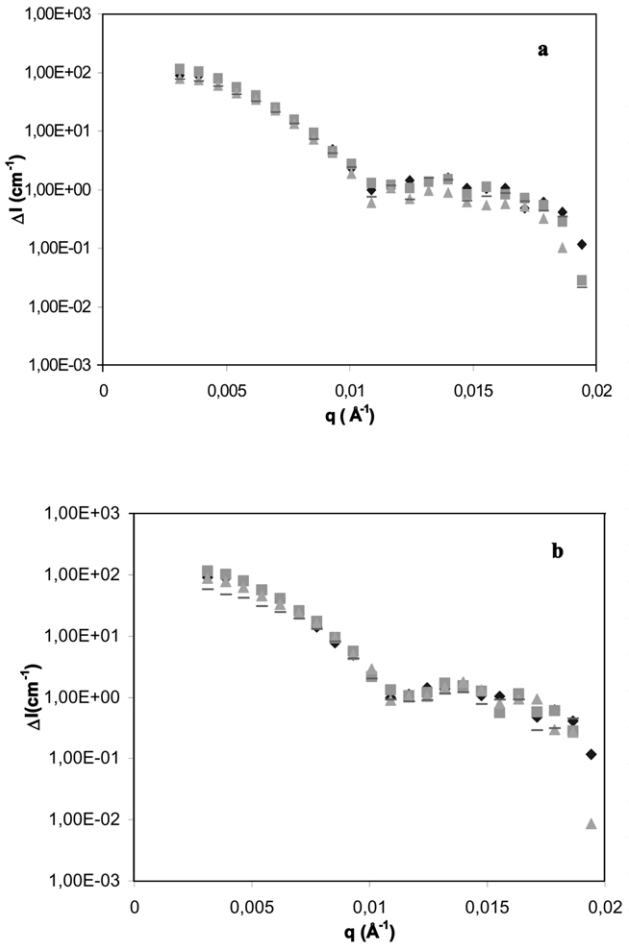

Fig. 10. Scattered intensity of 1% PS1 latex suspensions in H_2O/D_2O (82.4/17.6%) mixture in the presence of mono-functionalised (a) and di-functionalised (b) PEO: 0% (◆), 3% (▩), 5% (○), 10% (▲), and 20% (—) polymer.

Calculations were made with $R = 90$ nm and the latex density $d_l = 1.1$ g ml^{-1}.

Then, the available latex surface per polymer is $S_{pl} = 18 \pm 3$ nm^2.

If the polymer was adsorbed onto latex as a mono-layer keeping the same conformation as in solution, the surface which should be required for one molecule is $\pi R_g^2 \approx 13$ nm^2, R_g being the radius of gyration of a pure PEO of $\bar{M}_w = 16\,000$. ($R_g = 6$ nm as calculated by the power law [31] $R_g = 0.0215M^{0.583}$ (nm)). Thus, polymer molecules must be strongly stretched to cover a surface area of 15 nm^2, which corresponds to a radius of about 2.4 nm.

The order of magnitude for the average surface per macromolecules was obtained by Pham and Russel [19], for adsorption of an associative polymer close to our sample, on poly(methyl methacrylate) latex. From the theoretical models of de Gennes [34] and Alexander [35], it is possible to evaluate, as already done in Ref. [19], the thickness of the adsorbed layer:

$$\delta \approx L\left(\frac{\delta v}{6l^3}\right)^{1/3} \tag{19}$$

(L and l are, respectively, the polymer contour length and the Kuhn length, v is the excluded volume parameter and σ is the number of molecules per surface unit. A thickness of about 30 nm is expected from this expression.

(ii) With a concentration of 10% polymer, if one assumes that the amount of adsorbed polymer is the same as at the lower concentration, the excess free polymer is expected to form micelles which can self-assemble into a network as in pure water. The fact that the scattered intensity of the polymer in the presence and in the absence of latex may be interpreted as a compensation between two effects: at first the concentration of free polymer is lower than the reference concentration in pure water, which could induce a loss of scattered intensity; but secondly, as seen in Fig. 4, the intensity at q_{max} decreases upon increasing concentration, due to the PEO corona overlap.

In this solvent, the results seem to be compatible with the occurrence of polymer adsorption.

3.3.4. Mixture of H_2O/D_2O (82.4/17.6%) as solvent

In this solvent mixture, PEO is matched because its contrast is brought to zero, the scattering length density of the solvent having the same value as that of PEO (see Table 1). The aliphatic end-groups of PEO can be neglected, as their volume fraction is relatively very small. Thus, the scattered intensity corresponds to latex alone.

With the solution with 1% latex (w/w with respect to the solvent), the addition of polymer has little effect on the scattering curves (Fig. 10(a) and (b)). Di-functionalised PEOM seems to decrease to a greater extent—when compared to mono-functionalised PEOM—the fluctuations of concentration, but the effect remains rather small.

At low q values, for the solution containing 10% latex, the scattered intensity decreases significantly when M16C16 or D32C16 are added. The effect is small for the 3 and 5% solutions but changes by almost a factor of 10 for the higher polymer concentration. As the polymer is matched, we can say that the fluctuations of concentration of the latex particles decrease (Fig. 11(a) and (b)). Moreover, there is a noticeable appearance of a peak for 20% polymer at 0.006 and 0.008 Å^{-1}, with M16C16 and D32C16, respectively. Let us note that in Fig. 10 (1% latex), the scattered intensity curve exhibits a singularity in the same q vector range.

Qualitatively similar results were obtained with the commercial latex PS2 in the presence of D32C16, as shown in Fig. 12. For the two higher concentrations 10 and 20% of polymer, one finds again a peak at about 0.009 Å^{-1}. Curiously, the oscillations seem to become more pronounced in the presence of polymer.

Let us consider at first the behaviours observed with 10% latex. Relation (3) shows that the $S(q)$ factor can be obtained

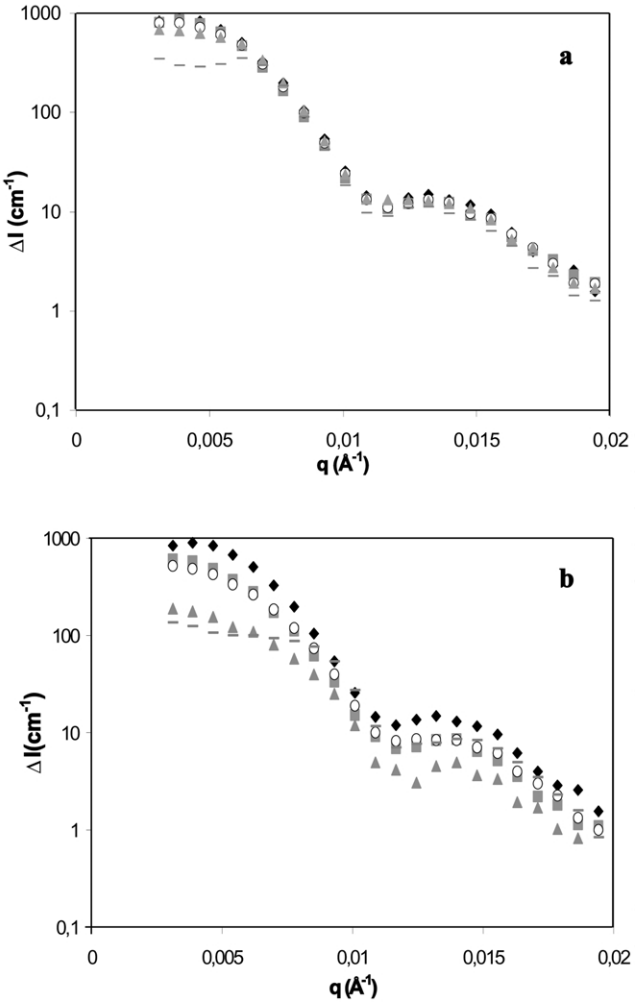

Fig. 11. Scattered intensity of 10% PS1 latex suspensions in H_2O/D_2O (82.4/17.6%) mixture in the presence of (a) mono-functionalised and (b) di-functionalised PEO: 0% (◆), 3% (▩), 5% (○), 10% (◬), and 20% (—) polymer.

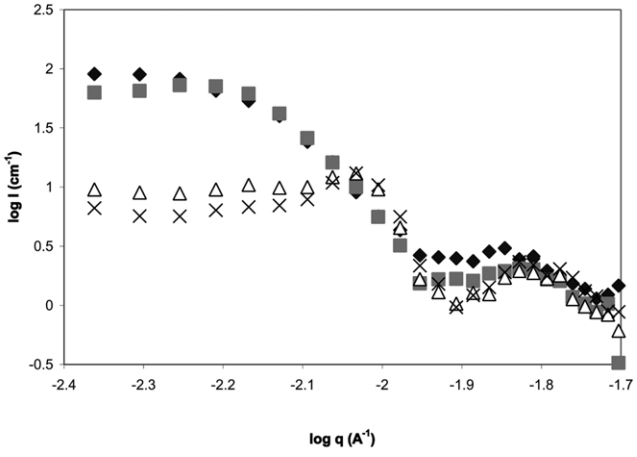

Fig. 12. Scattered intensity of 10% PS2 latex suspensions in H_2O/D_2O (82.4/17.6%) mixture in the presence of (a) mono-functionalised and (b) di-functionalised PEO: 0% (◆), 3% (▩), 10% (△), and 20% (×) polymer.

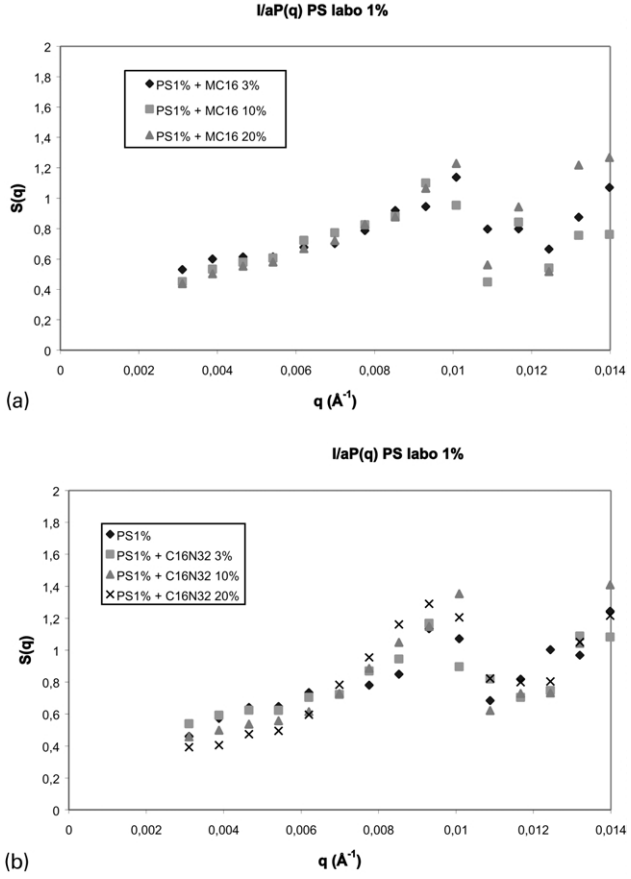

Fig. 13. Experimental function $S(q)$ for 1% PS1 latex suspensions with 0% (◆), 3% (▩), 10% (◬), 20% (×) of (a) mono-functionalised and (b) di-functionalised PEO.

by dividing ΔI by the form factor. In the presence of polymer and under these solvent conditions, it is obvious that $P(q)$ of latex must be exactly the same as in pure water. By using the expressions (5) and (7), we have obtained the variations of $S(q)$ versus q, as represented in Figs. 13 and 14. In the case of D32C16, a first peak is observed in all cases at about 0.008 $Å^{-1}$, followed by small peaks of lower intensity. The position of these peaks is independent of the polymer concentration with 10% latex (Fig. 14) and even if the peaks are less pronounced for 1% latex, they appear for the same q values. The first peak corresponds to an average distance between scattering centres: $d = 2\pi/q_{max}$. This distance is found to be equal to 80 ± 8 nm in the case of D32C16, which means that the particles are almost adjacent. It is slightly higher for M16C16 $d = 105 \pm 10$ nm, meaning that the particle surfaces are approximately 25 nm apart. The volume fraction deduced from d:

$$\Phi = V_1/d^3 \tag{20}$$

is then different for the two polymers: 0.52 ± 0.1 for D32C16 and 0.23 ± 0.08 for M16C16. The first value is much higher than the average volume fraction in the

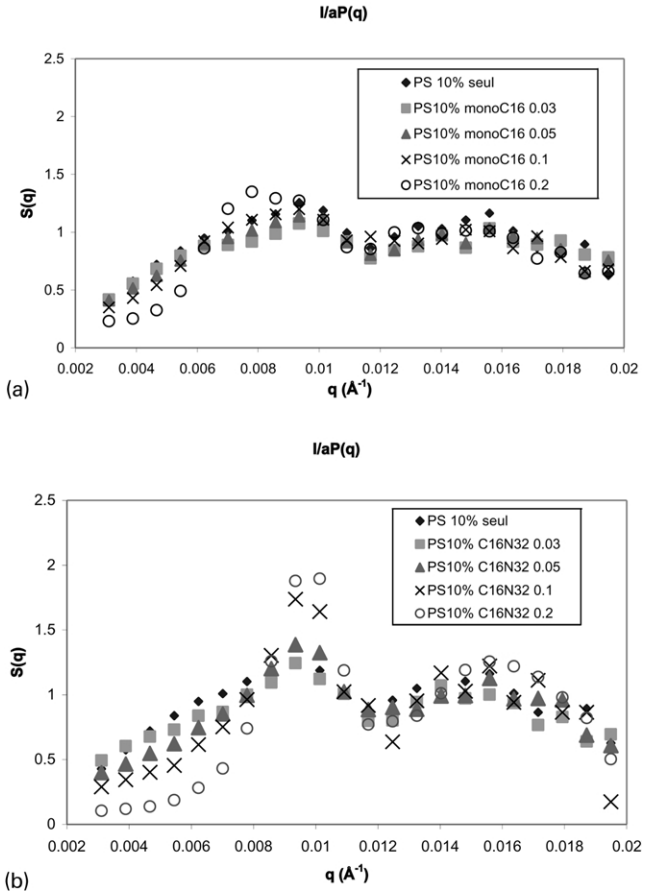

Fig. 14. Experimental function $S(q)$ for 10% PS1 latex suspensions with 0% (◆), 3% (■), 5% (▲), 10% (×), 20% (○) of (a) mono-functionalised and (b) di-functionalised PEO.

suspension ϕ_m (10%) but the second one is approximately twice ϕ_m. This result shows that these ternary systems contain latex aggregates even if they appear to be homogeneous. This could reflect the formation of soluble latex aggregates. The high value of volume fraction for D32C16 indicates that inside aggregates, the latex forms a dense array of particles. Fig. 15 shows, for the pure latex suspensions, a hard sphere based model derived from the scattering curve for 10% latex–20% M16C16 (using Eq. (7) for the form factor and Eq. (11) for the structure factor).

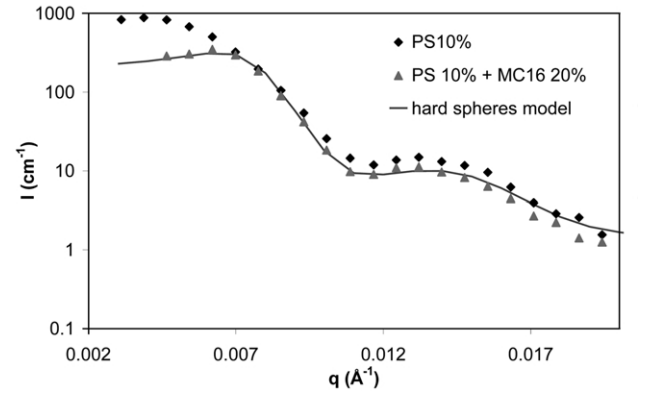

Fig. 15. Experimental results for PS1 10% (◆), PS1 (10%)/D32C16 (20%) (▲) and fitted curve (Eqs. (6)–(13), with $R = 400$ Å, $\Phi = 0.3$) for the system PS1 (10%)/D32C16 (20%).

Good results were obtained with the following set of parameters: $R = 400$ Å and $\Phi = 0.3$ in agreement with the previous observations. This confirms that the local volume fraction of latex in M16C16 solution is higher than ϕ_m.

Finally, the fact that the peak intensity increases upon increasing polymer concentration indicates that the fraction of latex involved in aggregation depends upon concentration and that this depletion effect becomes more and more pronounced with an excess of polymer.

4. Discussion

The neutron scattering results are consistent with the description of the ternary systems of latex/water/PEOM where a micro-phase separation occurs at least in the presence of di-functionalised PEO.

The general picture which is generally given for this type of ternary systems is schematised in Fig. 16(a): the latex particles are assumed to be uniformly distributed in a micellar solution of polymer. Parts of the hydrophobic end-groups are adsorbed onto the latex surface, the remainder forming the micelle cores. The appearance of a peak in the intensity curve scattered by latex alone may be due to repulsion between adsorbed corona. Our results show that this model may be more appropriate in the case of mono-functionalised polymer since the average distance between the latex particles, even in the presence of an excess of polymer, is not too high with respect to that expected for a homogeneous spatial distribution of latex.

In the case of the di-functionalised polymer, there is clearly a formation of latex aggregates corresponding closely to a close packing of particles. The two models represented in Fig. 16(b) and (c) may be considered: in the first one, the latex particles are gathered into aggregates through a bridging phenomenon. It seems quite normal to assume that the interactions between the di-functionalised PEO corona of latex are attractive. In fact, in this model, the inter-particular distance should be higher than that corresponding to close packing and be equal roughly to the sum of the particle diameter and the thickness of adsorbed layer. Nevertheless, the accuracy on the peak position in these experiments is not very good and it should be interesting to work with deuterated latex particles in order to increase the contrast factor and the measurement accuracy.

In the model in Fig. 16(c), the latex particles are adjacent and no more polymer is adsorbed. This behaviour could be due to the presence of a surfactant. Indeed, the stability of latex suspensions in pure water is due to adsorbed surfactant. One has to consider three types of interactions: latex/surfactant, latex/polymer and polymer/surfactant. It is

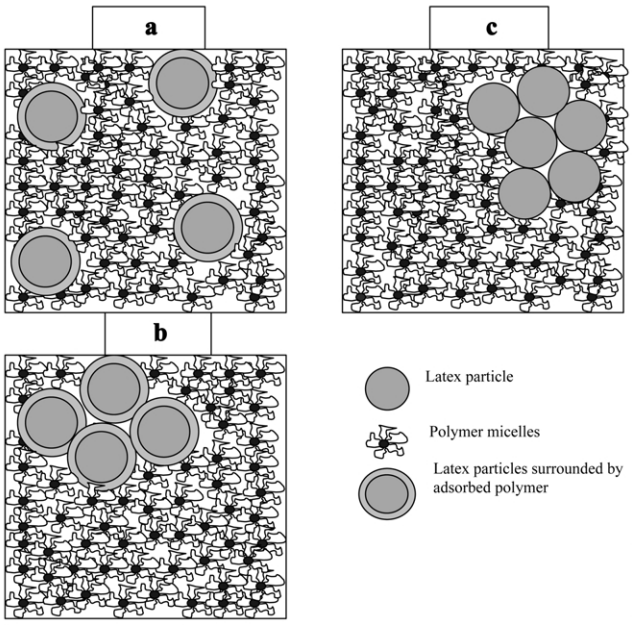

Fig. 16. Possible models of structure of the ternary systems (water/latex/PEOM).

known that hydrophobically end-capped PEO presents two sites of interaction for SDS: with the PEO chain [32] and with the aliphatic chains [33], the second one being considerably more important. It has been shown that there is a formation of mixed micelles at very low SDS concentrations when this surfactant is added in a polymer solution above its critical association concentration. According to the differences in the energies of the different processes, namely solubilisation of SDS in the micelle cores of the polymer, transfer of SDS molecules from the bulk to the surface and adsorption of polymer, it is possible that SDS is desorbed from the latex to be incorporated in the micelle cores. If the polymer is weakly adsorbed, then the latex becomes more stable. Nevertheless, it is difficult to understand why the mono-functionalised PEO behaves different from di-functionalised PEO. Besides (i) the fact that at low polymer concentration, the peak characteristic of the polymer disappears and (ii) the results of other types of experiments (DLS) which indicate polymer adsorption, are not consistent with this model. However, it is possible that surfactant plays a role.

5. Conclusion

Ternary systems of associative polymer/PS latex/water have been investigated under three different conditions:

In pure water, a decrease in the scattered intensity at small q, could be interpreted as a stabilisation effect due to polymer adsorption. One could believe that the PEO corona around latex particles may play the same repulsive role as observed for micelles or flower-like corona. Nevertheless, the experiments performed in solvents, where either latex or polymer is matched, show that this interpretation is applicable only to the case of mono-functionalised PEO.

In a solvent where the latex is matched, adsorption of polymer on latex seems to be confirmed when the polymer is not in a high excess with respect to the saturation concentration. At higher polymer concentrations, the peaks obtained in the presence and in the absence of latex are superimposed which indicates that the polymer available to form a micelle array is not significantly reduced by adsorption.

In a solvent where the polymer is matched, two cases have been observed: in the case of mono-functionalised PEO, the appearance of a peak consistent with the volume fraction of latex is consistent with the adsorption of polymer, the adsorbed corona being repulsive. In the case of di-functionalised PEO, the scattering curves can only be understood by considering that the latex aggregates almost correspond to a close packing of particles.

The method of variable contrasts, by varying the solvents, is a powerful tool enabling studies of these kinds of complex systems, even if definitive conclusions are difficult to draw. It is deemed necessary to increase the contrast factor and the accuracy of the measurements by using deuterated latex. Moreover, the fact that the latex particles are initially stabilised by an ionic surfactant increases the complexity of the system under study; it may be interesting to work with pure latex in the near future.

Acknowledgements

The authors thank L. Billon for his help in the preparation of D32C16 sample.

References

[1] Glass JE, editor. Polymers in aqueous media, performances through association. Advances in Chemistry Series 223. Washington, DC: ACS, 1989.
[2] Glass JE, editor. Hydrophilic polymers, performances and environmental acceptability. Advances in Chemistry Series 248. Washington, DC: ACS, 1995.
[3] Lundberg D, Glass E, Eley RR. J Rheol 1991;35:1255.
[4] Yekta A, Xu B, Duhamel J, Adiwidjaja H, Winnik MA. Macromolecules 1995;28:956.
[5] François J, Maitre S, Rawiso M, Sarazin D, Beinert G, Isel F. Colloid Surf 1996;112:251.
[6] Alami E, Rawiso M, Isel F, Beinert G, Binana Limbele W, François J. In: Glass JE, editor. Hydrophilic polymers, performance with environmental acceptability, Advances in Chemistry Series 248. Washington, DC: ACS, 1995. p. 343.
[7] Abrahmsen-Alami S, Alami E, François J. J Colloid Interface Sci 1996;179:20.
[8] Alami E, Almgren M, Brown W, François J. Macromolecules 1996;29:2229.

[9] Chassenieux C, Nicolai T, Durand D. Macromolecules 1997;30:4952.
[10] Gourier C, Beaudoin E, Duval M, Sarazin D, Maître S, François J. J Colloid Interface Sci 2000;230:41.
[11] Liu F, Frère Y, François J. Polymer 2001;42:2969–83.
[12] Ma Z. PhD Thesis, North Dakota State University, 1992.
[13] Tarng MR, Zeying M, Alahapperuma K, Glass JE. In: Glass JE, editor. Hydrophilic polymers. Performance with environmental acceptability. Advances in Chemistry Series 248. Washington, DC: ACS, 1995. p. 450.
[14] Richey BAB, Kirk EK, Eisenhart EK, Fitzwater S, Hook J. J Coat Technol 1991;63:31.
[15] Hulden M. Colloid Surf 1994;A88:207.
[16] Ma Z, Chen M, Glass JE. Colloid Surf A: Physicochem Engng Aspect 1996;112:163.
[17] Ouali L, François J, Pefferkorn E. J Colloid Interface Sci 1999; 215:36.
[18] Jenkins RD, Durali M, Silebi CA, El Aasser MS. J Colloid Interface Sci 1992;154:502.
[19] Pham QT, Russel WB. J Rheol 1998;42:159.
[20] Alahapperuma K, Glass JE. Prog Org Coat 1992;21:53.
[21] Kaczmarski JP, Glass JE. Macromolecules 1993;26:5149.
[22] Maitre S, Borisov O, François J. Submitted.
[23] Maitre S. PhD, University Louis Pasteur, Strasbourg, France, 1997.
[24] Morton M, Milkovich R. J Polym Sci, Part A 1963;1:443.
[25] Frot D. Private communication.
[26] Sensenacq C. DEA Report, University of Pau, France, 2000.
[27] Sensenacq C, Frot D, Roby F. In preparation.
[28] Benoit H, Higgins J. In: Neutron scattering.
[29] Percus JK, Yevick GJ. Phys Rev 1958;110:1.
[30] Beaudoin E. PhD, Université de Pau et des Pays de l'Adour, 2001.
[31] Denavand K, Selser JC. Nature 1990;343:739.
[32] Sabbadin J, Dayantis J, François J. Eur Polym J 1985;2:166.
[33] Binana Limbele W, Clouet F, François J. J Polym Colloid Sci 1992;33:1021.
[34] de Gennes PG. J Phys Lett 1975;36:255.
[35] Alexandra S. J Phys 1977;38:983.